

Rapid homogenization method for synthesis of core/shell ZnO/CdS nanoparticles and their photocatalytic evaluation

Suraksha Rasal^{1,2}, Priyesh V. More¹, Chaitanya Hiragond¹, Sunita Jadhav² and Pawan K. Khanna^{1*}

¹Nanochemistry/Nanomaterials Lab., Dept of Applied Chemistry, Defence Institute of Advanced Technology (DIAT), Govt. of India, Pune 411 025, India

²Department of Chemical Engineering, Bharati Vidyapeeth University, Katraj 411046, Pune, India

*Corresponding author. E-mail: pawankhanna2002@yahoo.co.in

Received: 01 December 2015, Revised: 11 January 2016 and Accepted: 25 March 2016

ABSTRACT

ZnO/CdS core-shell hetero nanostructures with different shell thickness have been successfully developed by a solution chemistry method employing rapid homogenization concept. The obtained core/shell nanoparticles were characterized by X-ray diffraction (XRD), field emission scanning electron microscopy (FESEM), energy dispersive X-ray analysis (EDX), FTIR, Raman, photoluminescence (PL), and UV-visible spectroscopy. All analytical and spectroscopic tools supported the formation of CdS shell over ZnO core. ZnO/CdS core-shell nanostructures were evaluated for their photocatalytic activity against methylene blue (MB), a common industrial water pollutant. It was observed that the ZnO/CdS core-shell nanostructures can effectively function as a photocatalyst under both UV and sunlight for degradation of MB. It was also observed that the degradation of MB was higher from core/shell nanostructures than the physical mixture of ZnO-CdS which was prepared separately. Copyright © 2016 VBRI Press.

Keywords: Homogenization; core-shell QDs; photocatalysis; solution chemistry; dye degradation.

Introduction

In recent years, the research in the field of photocatalysis has become attractive due to the increasingly serious environmental issues. The use of semiconductor materials as photocatalyst has attracted considerable importance due to their efficient degradations of pollutants [1, 2]. Zinc oxide (ZnO) and Titanium dioxide (TiO₂) have been often considered as the effective photocatalysts due to their ability to act in ultra-violet as well as marginally in the visible region up to about 400 nm. TiO₂ (bulk band gap of 3.2 eV) and ZnO (bulk band gap of 3.37 eV) have been thus studied extensively as photocatalysts because of their suitable band gap and high photocatalytic activity. TiO₂ can function only in Ultra violet (UV) region because of its large band gap energy of 3.2 eV. However, ZnO nanoparticles exhibit a few advantages over TiO₂ nanoparticles as the band gap of ZnO (3.37 eV) is slightly higher and tailoring of nano-structures in ZnO is simpler than TiO₂. Additionally, ease of crystallization and higher electron mobility makes it better photocatalyst than TiO₂ [3]. However, there are some disadvantages of using these semiconductor materials as photocatalysts because of not been able to utilize the energy available in the visible light region between 400-700 nm. These drawbacks can be overcome by employing appropriate strategy to improve the band-gap of the materials for the requirement in the visible region. Thus a possible coating of lower band gap material might be an appropriate alternate where it may pull the

higher band gap of the core to visible light and lower the band gap of the combined nano-structure at the same time be able to retain sturdy and robust nature of the core material. II-VI semiconductor nanoparticles have often been considered as potential coating materials due to their tunable band-gap in the entire visible region owing to their tunable particle size and surface properties favorable to absorption in the range of 400-700 nm. This offers a platform to the researchers to alter the band gap of semiconductor by appropriately managing the reaction conditions for controlling the size of the particles by virtue of optimum quantum confinement effects. These manipulations can be handful for creating composites nanoparticles, core-shell nanoparticles, nanorods, nanoarrays, nanowires, and doped metals with tailored band-gap in semiconductor [4-9]. Many methods are followed by the researchers to develop nanoparticles based photocatalyst, which are sol-gel, SILAR, spin coating, precipitation, sonochemical, thermal deposition, homogenization, chemical deposition etc. The chemical and physical properties of different photocatalyst depend not only on their sizes and morphologies but also on their synthesis techniques. [10-13]. Core-shell nanoparticles have variety of applications as compared to their individual single nanostructure thus the major advantage of making core-shell structures is alteration of the charge, functionality, and reactivity of the surface due to coating of one material over another [14-15]. To enhance

photocatalytic efficiency of metal-oxide semiconductors in the visible region, it is necessary to couple them with a lattice matched photo-sensitizer which has narrow/mid band gap. Hence, developing a novel photocatalyst, such as metal oxides (e.g. ZnO) and cadmium sulphide (e.g. CdS) can be advantageous to get response in both UV and visible region [16-19]. CdS is one of the most important II-VI semiconductors used in various photoelectronic devices [20]. CdS with direct bulk band gap energy of 2.42 eV is one of the first discovered semiconductors which have most applications in photocatalysis, solar cell, gas sensor, optoelectronic devices etc [21-22]. Usually, the common methods to increase the utilization of visible light and enhancing the separation of charge carriers are doping of metal oxides or using a sensitizer. Among the most widely used inorganic semiconductor sensitizers, CdS is therefore considered to be the most suitable visible light sensitizer for ZnO [23-25]. Also, ZnO is relatively non-toxic material, a core-shell system of ZnO and CdS nanostructures is expected to be highly effective [26-27]. Use of only chalcogenide based photocatalyst may pollute the environment as also their stability is not ascertained over a long period of time. Keeping this in mind, we herein explore a simple ZnO/CdS core/shell nanostructure system which is synthesized by a two-step method where ZnO is first prepared by sol-gel method and CdS shell is grown over it *via* solution method by ultra-fast homogenization process employing 3-mercaptopropionic acid as a surfactant. The so-prepared core-shell structure has been characterized by various modern tools and their photocatalytic performance against methylene blue dye is studied.

Experimental

Materials

"CdCl₂.H₂O (95%) was commercially purchased from Qualigens Fine chemicals, Na₂S.H₂O was purchased from Hi Media laboratories (India), 3-mercaptopropionic acid (MPA; +99 %) from Sigma Aldrich (India), ZnNO₃.6H₂O (99 %) was purchased from highly purified laboratory chemicals (India), Homogenizer IKA (Germany) model-T25DS22, UV-CABINET Bio-Technics (India) model no. – BTI-49 was used for the experiments. UV-visible absorption spectra were obtained at room temperature using analytikjena SPECORD@210plus spectrophotometer and photoluminescence (PL) spectra were obtained using Cary-Eclipse Fluorescence spectrophotometer of Agilent Technology. The excitation wavelength for PL measurement was set to 350 nm. Powder X-ray diffraction (XRD) patterns were acquired using Bruker D8 Advance diffractometer with Cu K α radiation (1.5405 \AA) at 45 kV and 40 mA. FESEM and EDAX were performed using supra 40, Carl Zeiss Pvt. Ltd. Instrument. All the measurements were performed under atmospheric conditions. Fourier transform infrared (FTIR) spectra were obtained using a Perkin Elmer Spectrum-Two infrared spectrometer in the range of 4000 to 400 cm⁻¹. Raman spectra were recorded using EZ Raman spectrometer and are presented in the range 600 to 100 cm⁻¹. Surface topology was studied using Atomic force microscope (Asylum Research MFP3D). The photocatalytic activity of

the catalyst (ZnO/CdS core/shell nanoparticles) was performed under sunlight as well as under 365 nm fixed wavelength UV lamp (8 watt)."

Synthesis of ZnO nanoparticles

Synthesis was performed by reported method [28]. In a typical experiment, water and Starch was used as a solvent and capping agent respectively. 1.0 gm of zinc nitrate was added in to the 50 ml distilled water at room temperature under vigorous stirring and pH was maintained at 8 by using sodium hydroxide. The reaction mixture was then kept at 60 °C at 300 rpm for 3 hrs. The white precipitate of Zn(OH)₂ was washed with ethanol twice and dried at 60 °C temperature in the oven for 24 hrs to obtain ZnO nanoparticles.

Synthesis of CdS nanoparticles

The CdS nanoparticles were synthesized by sonication method. Water and 3-mercaptopropionic (MPA) acid was used as a solvent and capping agent respectively. 1.0 gm of CdCl₂.H₂O and 0.5 gm of MPA were mixed with 50 ml distilled water at room temperature and was continuously sonicated for 5-10 min. To, this mixture aq. Na₂S.H₂O was added drop wise. The reaction mixture so-generated was further sonicated for 15 minutes. The final precipitate was washed 2-3 times with ethanol and water and was dried at 60 °C in oven for 24 hrs.

Synthesis of core-shell ZnO/CdS nanoparticles

First, the so-prepared ZnO nanoparticles (1gm) were re-dispersed in water with the use of homogenizer. The shell CdS layer was generated around ZnO by using CdCl₂.H₂O and Na₂S.H₂O along with 3-mercaptopropionic acid in such a manner so as to generate 1:1, 1:1.5 and 1:2 ratios between ZnO core and CdS shell. The overall method of formation of CdS shell on ZnO core is as described in section 2.3. The obtained off-white precipitate was washed with ethanol/water and then dried at 60 °C in the oven for 24 hrs.

Preparation of physical mixture of ZnO/CdS

The physical mixture of ZnO and CdS was prepared by physically mixing respective nanoparticles in 1:1 ratio in a mortar pestle. The so-prepared mixture was evaluated for photocatalytic activity.

Results and discussion

The current work describes a simple ZnO/CdS core/shell nanostructure system which is synthesized by a two-step method where ZnO is first prepared by sol-gel method and CdS shell is grown over it by rapid homogenization method. The as-synthesized ZnO/CdS core/shell nanoparticles were compared with a physically prepared ZnO/CdS nanocomposite powder for its photocatalytic activity against degradation of methylene blue dye. For this purpose, 3-mercaptopropionic acid (MPA) was used a capping agent to grow a CdS shell on pre-synthesized core ZnO nanoparticles. The core ZnO nanoparticles were synthesized by well-known sol-gel method using starch as capping agent. The shell thickness was varied by increasing

the concentration of Cd and S precursors and three samples with varied theoretical ZnO: CdS ratios were prepared. These samples are labeled as S1 (1:1), S2 (1:1.5) and S3 (1:2). Typical reaction process and formation of core-shell nanostructure is presented in Fig. 1.

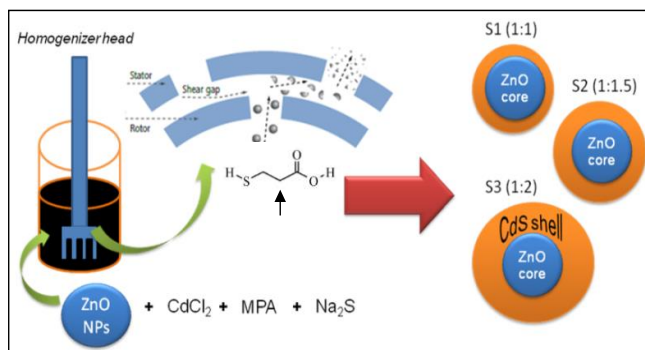


Fig. 1. Formation of core-shell nanostructures by rapid homogenization method.

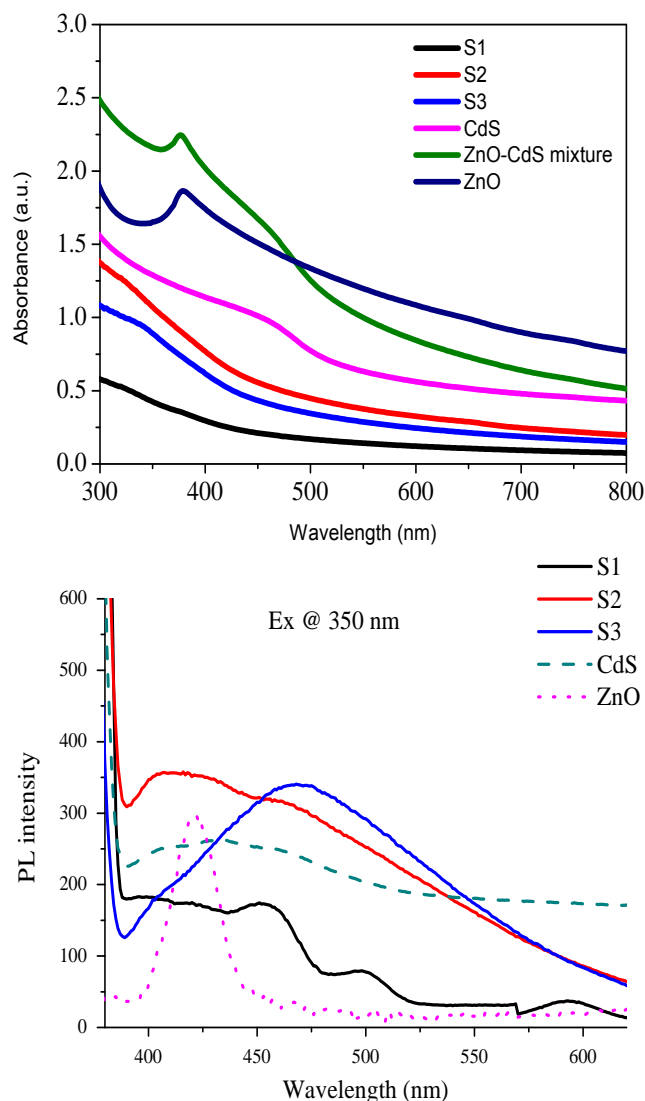


Fig. 2. a) UV-Visible absorption spectra of ZnO, CdS, Physical mixture and core-shell ZnO/CdS nanoparticles (S1 (1:1), S2 (1:1.5), S3 (1:2) and b) PL spectra of ZnO, CdS and core-shell ZnO/CdS S1 (1:1), S2 (1:1.5), S3 (1:2).

The UV-visible absorption spectra of ZnO/CdS core shell nanoparticles have been depicted in Fig. 2a along with respective nanoparticles. The as-synthesized core-shell ZnO/CdS showed absorption covering both UV and visible region. The rising absorption profile of all the three samples showed featureless pattern but the absorption intensity increased 5-6 folds between 300-700 nm. The absorption profile of physical mixture of ZnO/CdS showed two reasonably clear bands at 372 (3.33 eV) nm and 455 nm (2.72 eV) representing ZnO nanoparticles and CdS quantum dots. The absorption value of CdS alone was found to be about 450 nm (2.75 eV). The combined core-shell particles significantly differ in their absorption pattern in comparison to ZnO as well as CdS alone. Similarly, absorption properties also differ from the physically prepared ZnO/CdS nanocomposite. Such an observation primarily hints towards the formation of core-shell like structures composed ZnO and CdS. Thus it was observed that the band gap of ZnO/CdS core shell nanoparticles covers the energy range from 2.7 - 3.33 eV indicating good possibility of this composition to be an effective photocatalyst in both UV and Visible region.

The optical properties of nanomaterials are known to alter after formation of core-shell structures. The introduction of shell material over the core modifies the optical properties of the core [1]. The surface related defects on the core as well as in the interface of the core and shell may also play a major role in defining the optical properties of these materials. We assume that the as-synthesized ZnO/CdS core/shell nanoparticles must possess such surface related defects as the synthesis condition where relatively mild and formation of nanocrystalline, defect free nanoparticles would be difficult to obtain. To study such surface related defects on the QD surfaces, study of Photoluminescence (PL) was conducted and the results are shown in Fig. 2b. All the emission spectra were recorded with excitation energy of 350 nm. The PL spectra revealed a broad profile for all the three ZnO/CdS samples with various shell thickness and are compared with individual ZnO and CdS PL spectra. The profile was comprised of multiple peaks for samples S1 and S2 however a broad profile was observed for S3. Since the shell thickness is higher in sample S3, the broad profile predominantly relates CdS, further supporting the formation of core-shell structure. The surface related defects may arise from the combine effect of Cd-S bond due to presence of thiol capping (from MPA) and uncoordinated S-atoms from CdS shell surface. The deconvolution of PL peaks resulted in presence of successive peaks which could be due to non-radiative recombinations between photoexcited holes and electrons in the mid-gap states (Fig. S1). The multiple emission profile is also attributed to the charge recombination from surface mid-gap states that evolve from the presence of non-coordinated surface sulphur sites (dangling bonds) from CdS shell and Cd-S bond from CdS-thiol interaction. The presence of thiol group was identified by FTIR spectroscopy also (Fig. 3b). Careful analysis indicates that where the ratio between ZnO and CdS is 1:1, the emission profile relates to both from ZnO as well as from CdS which moves more towards the CdS upon increasing the ratio

from 1:1 to 1:1.5 and 1:2. The broad profile is due to the well-known surface related defects present in the quantum dots structures [29].

These surface related defects may play a vital role in the desired photocatalytic properties. Photoluminescence is the result of direct radiative recombination, lower recombination of generated carriers causes the decrease of light emission intensity which simultaneously increases the photocatalytic activity of the semiconductors. The weak excitonic PL intensity relates to higher photocatalytic activity because of electron transfer from ZnO to CdS during photonic excitation. This probability might enhance with respect to ideal CdS thickness around ZnO thus, it is likely to be catalyzing the process in the UV as well as visible light region.

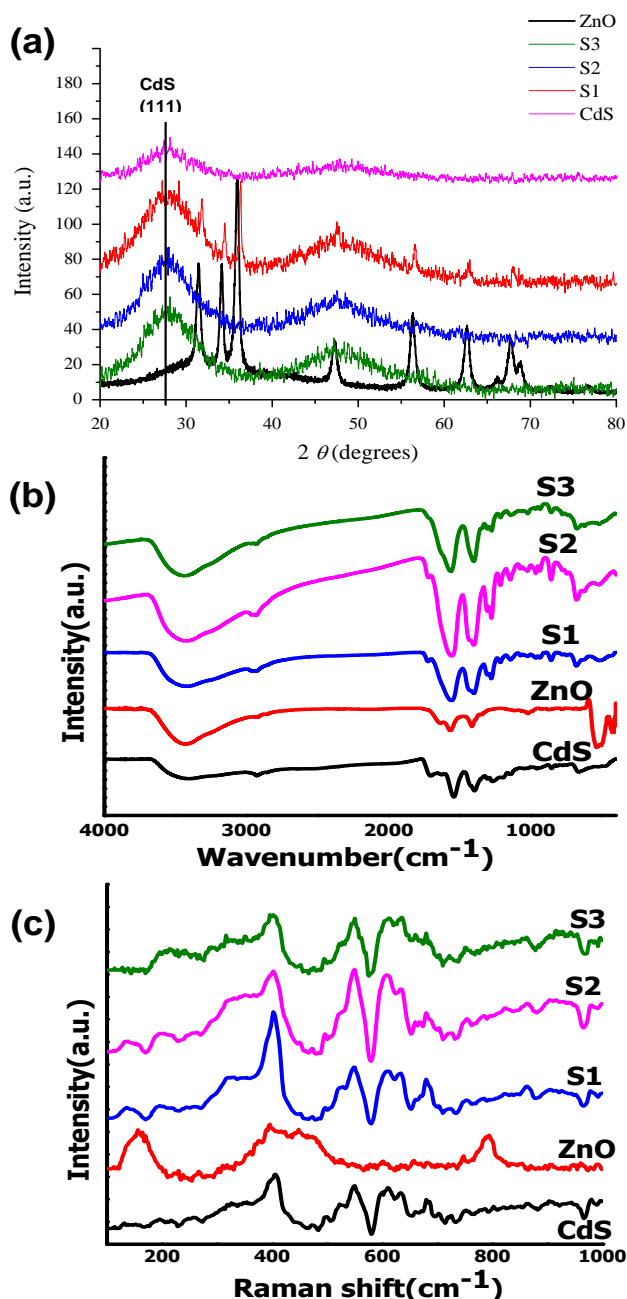


Fig. 3. a) XRD pattern of ZnO, CdS and ZnO/CdS core-shell nanoparticles, b) FTIR and c) Raman spectra of core-shell ZnO/CdS nanoparticles with varying shell thickness.

X-ray diffraction pattern of a ZnO/CdS core/shell nanoparticles is shown in **Fig. 3a** where the diffraction peaks can be indexed to the spherical ZnO/CdS core shell structure. In total, seven diffraction peaks corresponding to the (100), (002), (101), (102), (110), (103), (200), (112) and (201) planes of the hexagonal (wurtzite) crystal structure of ZnO (S1 sample) were observed. The broad diffraction peak, corresponding to the (111) plane of the CdS phase could be due to overlap of several characteristic peaks of CdS possibly because of amorphous nature of the CdS layer. The disappearance of characteristic peaks of ZnO in sample S2 and S3 suggest that CdS shell thickness is relatively higher thus suppressing the long range diffraction intensity of ZnO. This confirms that shell thickness increased with increasing the concentration of Cd and S precursors with respect to ZnO and is in line with the observation made from UV-Visible and PL spectroscopy. Due to very broad nature, it was not considered appropriate to apply FWHM concept for calculation of crystallite size using Scherer equation.

Fig. 3b shows the FTIR spectra of the samples with different shell ratio with respect to core ZnO. Since the shell CdS is passivated by MPA, it may be identified by the presence of its functional groups from IR spectrum. MPA has C=O from the carboxylate group and has C-S bond from thiol. The peaks at 1350 and 1590 cm^{-1} are characteristics of C-S and C=O bonds. The other peaks between 600 - 1200 cm^{-1} are due to C-H symmetric and asymmetric mode of vibrations. Broad profile between 3000 - 3600 cm^{-1} is due to presence of OH from the surfactant. The vibration band for Zn-O and CdS were observed at ~500-700 cm^{-1} . All the core-shell samples show increasing sharpness of peaks with increase in CdS shell thickness.

The Raman spectra of core-shell ZnO/CdS nanoparticles showed a major peak at 410 - 25 cm^{-1} with one strong peak with a weak shoulder associated with it. This peak may arise due to combination of both the E1 (TO) and E2 (High) modes of ZnO. All other peaks due to A1 modes and due to zone boundary phonons (3E2H - E2L) were not clearly observed possibly due to over coating of ZnO by CdS. **Fig. 3c** is Raman spectra of synthesized ZnO/CdS which confirms the presence of CdS shell over ZnO core. The weak Raman signals near 300 cm^{-1} can be related to longitudinal optical (LO) phonon peak and its overtones. The peak obtained is too broad and hence reflecting the presence of many photons of CdS. The higher order Raman features are clearly present near 410 - 25 cm^{-1} . These peaks are possibly shifted with reference to the observations made by others and this could be attributed to the formation of alloy at the interface of ZnO and CdS [30]. The Raman scattering observed in between 500-600 cm^{-1} can also be attributed to the combination of various mode of vibration in e.g. CdS_{LO+SO}, CdS_{alloy}, and CdS_{LO+alloy} with ZnO [31-32].

The morphology of ZnO/CdS nanoparticles was examined by FESEM (**Fig. 4a-c**) and AFM (**Fig. 4d**). The as-prepared ZnO/CdS nanoparticles showed highly aggregated spherical nanoparticles. Based on XRD findings, it was assumed that the size of CdS shell is relatively thick as the peaks for ZnO suppressed or disappeared under the matrix of CdS.

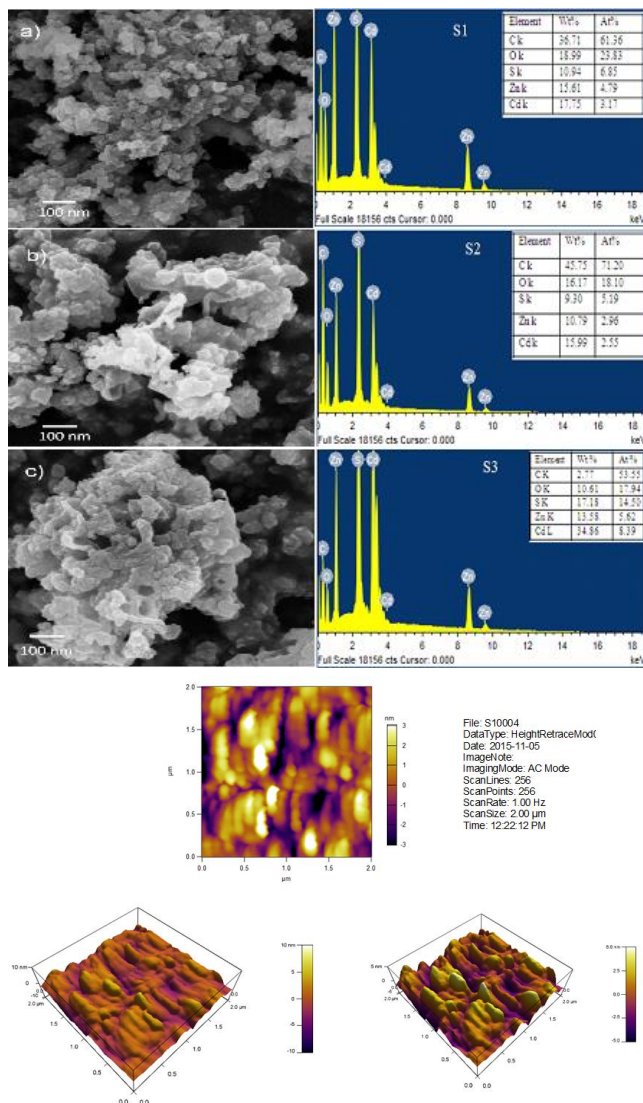


Fig. 4. FE-SEM images of ZnO/CdS core/shell nanoparticles a) S1 (1:1), b) S2 (1:1.5) and c) S3 (1:2) and their corresponding EDAX analysis (inset) and d) AFM Images of ZnO/CdS (1:1) core-shell nanostructure.

This hypothesis is well supported by FESEM images as dense, amorphous matrix of CdS is clearly visible, especially for S2 and S3 samples. For comparison purposes, SEM image of ZnO core and S3 sample is presented in **Fig. S2** where change in the surface morphologies of the samples after growth of amorphous shell on crystalline ZnO core is clearly observed. The EDAX analysis confirmed the presence of ZnO and CdS as the respective elements were detected in the samples. An increase in weight percent of Cd and S (from S1 to S3) was observed with respect to the concentration of ZnO which further supports the claim that shell thickness was increased by increasing the concentration of Cd and Se precursors. **Fig. 4d** shows AFM images of the sample where ZnO: CdS ratio was 1:1. It is seen from the figure that surface topology was slightly non-spherical which may be considered appropriate as there was hint of such morphology by FESEM also. The coating of CdS around the ZnO particles may not be therefore uniform and maximum coating might occur at the base of such slightly deformed particle due to density factor during solution

processing of the core-shell nanostructure formation. Overall, it appears to be smooth densely populated nanoparticles with flat and pointed valley type appearance. The diameter and the depth of the cluster from AFM in understood to be about less than 6 nm.

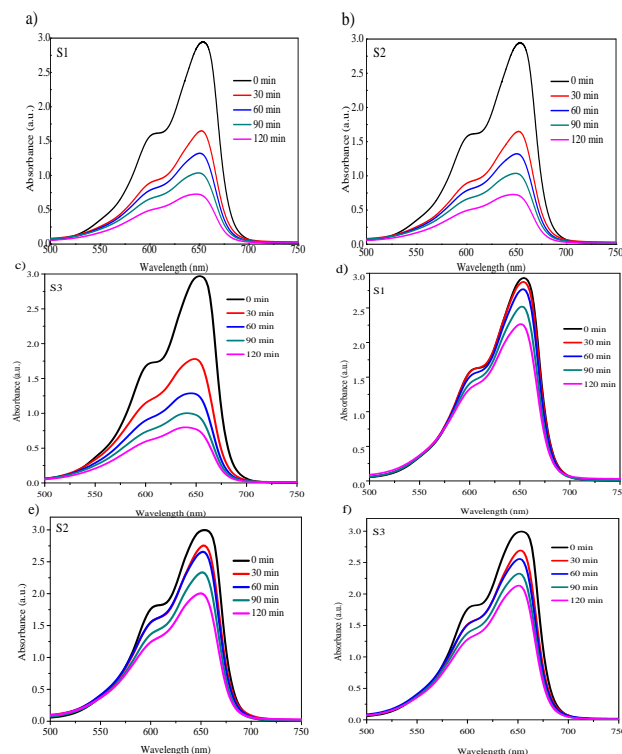


Fig. 5. The photocatalytic performance of methylene blue (20 ppm) using photocatalyst a), b) and c) under sun light and d), e) and f) under UV light respectively.

The measurement of particle size distribution (**Fig. S3**) was conducted by Laser based dynamic light scattering technique (DLS). The dilute solution of the sample was appropriately dispersed in dimethylformamide (DMF) by sonication for 1-3 minutes followed by slow centrifugation. The supernatant was then taken for the DLS analysis. It was observed that the sample S1 had the narrower size distribution in comparison to S2 and S3. This may be due to formation of wide size CdS layer around ZnO and as the shell thickness increased the distribution broadened.

Photocatalytic activity and degradation of MB

The photocatalytic activity of the catalyst (ZnO/CdS core/shell nanoparticles) was performed by two ways i.e. under sunlight and under UV lamp (8 watt; $\lambda=365$ nm). For a typical photocatalytic experiment, 25 mg of the photocatalyst was dispersed in 50 ml aqueous solution of methylene blue (20 ppm or 10 ppm) and stirred in dark condition. Later, the beaker was kept under sunlight for 2 hrs and aliquots (10 ml) were withdrawn at a periodic time intervals. The aliquots were centrifuged and 3 ml solution was taken from the supernatant for UV-visible spectroscopy monitoring. For the experiments under UV lamp, similar conditions were practiced. The experiments were also conducted using pure CdS nanoparticles, ZnO-CdS physical mixture. The mechanism of dye degradation can be explained by the mechanism reactive

oxidizing species (ROS) by the photocatalyst under the influence of sunlight or UV light. In this process reactive oxidizing species were produced in two steps. In the first step, dissociative adsorbed H₂O molecules are oxidized by the photogenerated holes and in the second step the photoexcited electrons reduces the electron acceptor.

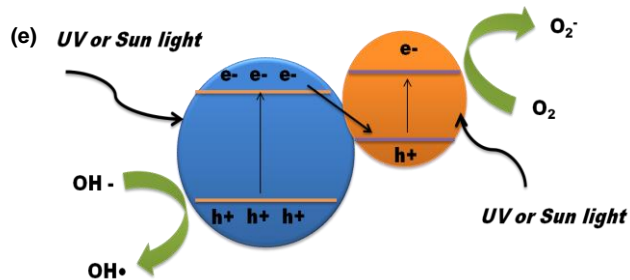
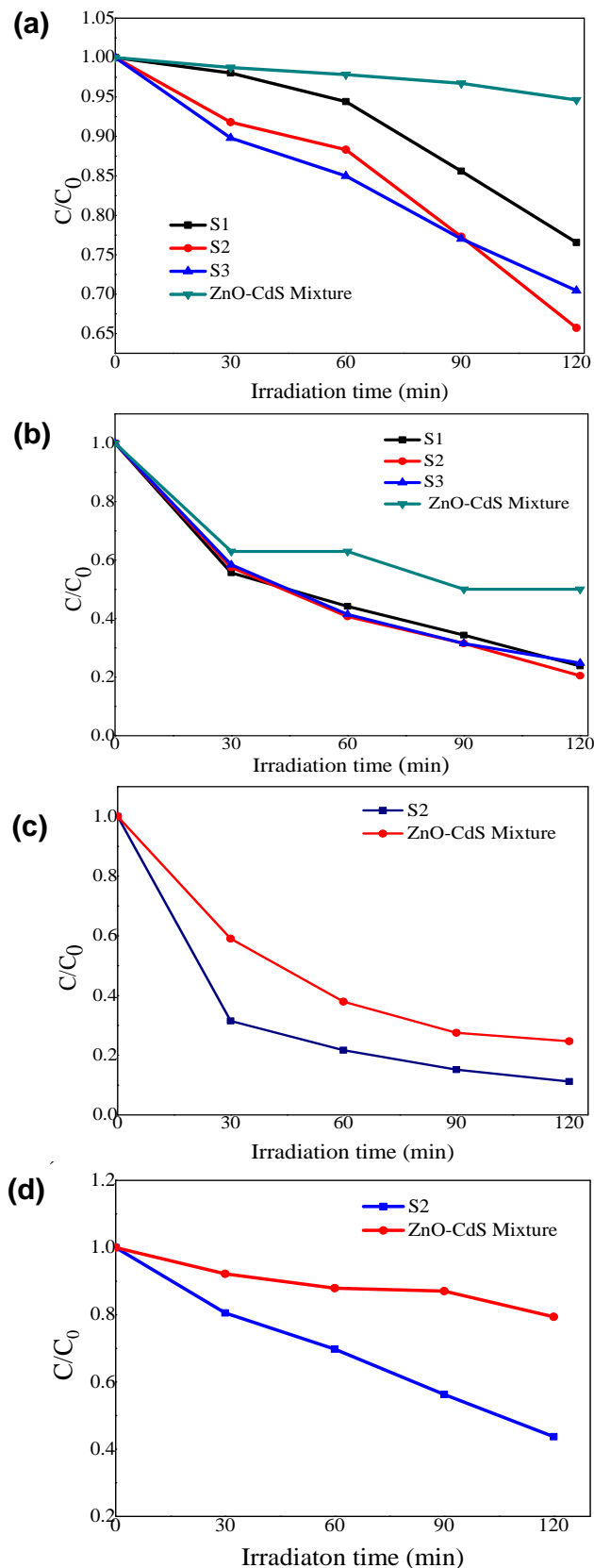


Fig. 6. Degradation rate of methylene blue (20 ppm) using photocatalyst a) under sunlight and under b) under UV light respectively, and comparison of S2 and physical mixture for degradation of methylene blue (10 ppm) c) under sun light and d) UV light respectively and e) Schematic representation of photocatalysis mechanism for MB degradation



Typically, the reactive photogenerated holes react with adsorbed OH⁻ on the catalyst surface to form hydroxyl (OH[•]) radicals and the excited electrons in the conduction band move to the surface and further react to the surface-adsorbed oxygen producing superoxide anion radicals (O₂^{•-}). These superoxide anion radicals react with H₂O to produce OH[•]. These radicals are identified as act as one of the most powerful oxidizing species. Both the radicals formed here react with MB to decompose it [33-35]. Methylene blue has a characteristic absorption peak in the region of 550-700 nm. The intensity of this peak decreased considerably when methylene blue was mixed with the photocatalyst in aqueous medium. The decrease in intensity indicated that the dye was degrading in the presence of photocatalyst under the influence of sun light or UV-light (Fig. 5).

It was observed that, the degradation of MB was higher under sun light as compared to UV light. The natural sunlight comprises of 2 - 4 % of UV light along with the large amount of visible light (~46 %) [36]. Thus, natural sunlight can be considered ideal energy source for core-shell ZnO/CdS photocatalyst as the ZnO core can absorb the near UV light to excite its electrons which can get transferred to CdS shell and also produce OH[•] radicals in the process. Additionally, The CdS shell can absorb the visible light to undergo photo-excitation which will effectively generate O₂^{•-} radicals [37]. However, considering the fact that we were dealing with a fix wavelength of 365 nm in UV range, the efficiency obtained under UV lamp can be considered as significant.

The possible mechanism is presented in Fig. 6. The concentration of MB is proportional to absorbance according to the Beer-Lambert Law and hence the degradation efficiency can be calculated using:

$$R = (C_0 - C) / C_0 \times 100 \%$$

where, C₀ and C are the concentration of methylene blue at the reaction time 0 and t seconds respectively. The highest degradation obtained by S2 sample under sunlight was 81 % and under UV light was 35 %. All the three samples (S1, S2 & S3) showed more than 70 % degradation for 20 ppm MB concentration under sunlight and more than 20 % degradation under UV light (Fig. 6). The better performance of S2 sample could be due to the optimum shell thickness of CdS as compared to S1 and S2. The shell

thickness in S3 sample could be thin as evident from XRD while it would be too thick in S2 sample. The reason for such higher efficiency could be the result of the combining of photoexcited electrons from the lower conduction band minima (CBM) of ZnO semiconductor with holes in the higher valence band maxima (VBM) of CdS. The thin shell layer will not allow the efficient combination as CdS concentration could be very low (S1 sample).

Alternatively, thick shell layer will mean higher concentration of CdS which results in larger distance to travel for the photoexcited electrons towards the surface to interact with the dye or the surface adsorbed oxygen. Interestingly, for 20 ppm MB solutions, the physical mixture of ZnO and CdS nanoparticles showed only 51 % degradation efficiency under sun light this was much lower in comparison to ZnO/CdS core/shell nanoparticles. The degradation efficiency of physical mixture under UV light was also relatively low (~5 %) as compared to ZnO/CdS core/shell nanoparticles (25-35 %). Similarly, for 10 ppm MB solutions, the ZnO/CdS core/shell nanoparticles showed ~85 % degradation efficiency in sunlight as compared to ~74 % shown by its physical mixture (Fig. S4). It was clearly evident that ZnO/CdS core/shell nanoparticles (S1, S2 and S3) were more efficient in MB degradation than its physical mixture. The reason for this could again be the higher combination of photoexcited electrons from the lower conduction band minima (CBM) of ZnO semiconductor with holes in the higher Valence band maxima (VBM) of CdS. These combinations will be highly enhanced in core/shell type structures as the interface (ZnO/CdS) area available will be more and defined in comparison to the ZnO and CdS physically mixed sample. However, the performance of the physical mixture improved for 10 ppm MB degradation but it was still lower than the ZnO/CdS core/shell nanoparticles. The present ZnO/CdS core/shell photocatalyst gives much better efficiency when compared with some of the commercial photocatalyst such as P25 (TiO₂) and ZnO where the reported degradation of MB was 10-60 % and 75 % respectively [38-39].

Conclusion

In summary, ZnO/CdS core-shell nanoparticles were synthesized successfully *via* solution chemistry method in aqueous medium by rapid homogenization method. The nanoparticles showed high photocatalytic activity due to the effective charge transfer between two coupled semiconductors. The as-synthesized samples were thoroughly characterized by UV-visible, PL, FTIR and Raman spectroscopy, SEM and XRD to verify the core/shell formation and shell thickness. In order to explore the photocatalytic behavior of the as-synthesized samples we successfully demonstrated the degradation of methylene blue in its presence. The synthesized ZnO/CdS nanoparticles demonstrated high photocatalytic activity under direct sunlight (81.28 %) however the same was much lower when 8Watt UV lamp was used (35.82 %) for the degradation of methylene blue in aqueous solution.

Acknowledgements

SR is thankful to Principal, BVCOE for permission to undertake a project

work at DIAT, Pune. PM thanks DST (PROJECT NO. IFA-13-PH68), Govt. of India for financial support. PKK thanks Vice-Chancellor DIAT, Pune for encouragement.

Reference

- Wei, H.; Wang, L.; Li, Z.; Ni, S.; Zhao, Q. *Nano-Micro Letters* **2011**, *3*, 6.
DOI: [10.3786/nml.v3i1.p6-11](https://doi.org/10.3786/nml.v3i1.p6-11)
- Stengland, V.; Kralova, D. *International Journal of Photoenergy* **2011**, *1*.
DOI: [10.1155/2011/532578](https://doi.org/10.1155/2011/532578)
- Aby, H.; Kshirsagar, A.; Khanna, P. K. *J Mater Sci Nanotechnol* **2015**, *3*, 302.
- Yang, Z.; Guo, L.; Zu, B.; Guo, Y.; Xu, T.; Dou, X. *Advanced Optical Materials* **2014**, *8*, 737.
DOI: [10.1002/adom.201470050](https://doi.org/10.1002/adom.201470050)
- Jana, T. K.; Pal, A.; Chatterjee, K.; *Journal of Alloys and Compounds* **2014**, *583*, 510.
DOI: [10.1016/j.jallcom.2013.08.184](https://doi.org/10.1016/j.jallcom.2013.08.184)
- Maurya, A.; Chauhan, P. *Material characterization* **2011**, *62*, 382.
DOI: [10.1016/j.matchar.2011.01.014](https://doi.org/10.1016/j.matchar.2011.01.014)
- Vaidya, S.; Patra, A.; Ganguli, A. K. *Collides and surfaces A: Physicochem. Eng. Aspects* **2010**, *363*, 130.
DOI: [10.1016/j.colsurfa.2010.04.030](https://doi.org/10.1016/j.colsurfa.2010.04.030)
- Kandula, S.; Jeevanandam, P. *J. Nanopart Res.* **2014**, *16*, 1.
DOI: [10.1007/s11051-014-2452-9](https://doi.org/10.1007/s11051-014-2452-9)
- Kuriakose, S.; Satpati, B.; Mohapatra, S. *Advanced Materials Letters.* **2015**, *6*, 217.
DOI: [10.5185/amlett.2015](https://doi.org/10.5185/amlett.2015).
- Kuriakose, S.; Satpati, B. and Mohapatra, S. *Physical Chemistry Chemical Physics* **2015**, *17*, 25172.
DOI: [10.1039/C5CP01681A](https://doi.org/10.1039/C5CP01681A)
- Mishra, Y. K.; Kaps, S.; Schuchardt, A.; Paulowicz, I.; Jin, X.; Gedamu, D.; Freitag, S.; Claus, M.; Wille, S.; Kovalev, A.; Gorb, S. N.; Adelung, R. *Particle & Particle Systems Characterization* **2013**, *30*, 775.
DOI: [10.1002/ppsc.201300297](https://doi.org/10.1002/ppsc.201300297)
- Mishra, Y. K.; Kaps, S.; Schuchardt, A.; Paulowicz, I.; Jin, X.; Gedamu, D.; Wille, S.; Lupan, O.; Adelung, R. *Kona powder and particle journal* **2014**, *31*, 92.
DOI: [10.14356/kona.2014015](https://doi.org/10.14356/kona.2014015)
- Zhang, Y.; Zhou, H.; Liu, S. W.; Tian, Z. R.; Xiao, M. *Nano Letters* **2009**, *9*, 2109.
DOI: [10.1021/nl900622q](https://doi.org/10.1021/nl900622q)
- Reimer, T.; Paulowicz, I.; Roder, R.; Kaps, S.; Lupan, O.; Chemnitz, S.; Benecke, W.; Ronning, C.; Adelung, R.; Mishra, K. *Applied Material Interfaces* **2014**, *6*, 7806.
DOI: [10.1021/am5010877](https://doi.org/10.1021/am5010877)
- Ramasamy, V.; Anandan, C.; Murugadoss, G. *Material Science in Semiconductor Processing* **2013**, *16*, 1759.
DOI: [10.1016/j.mssp.2013.06.027](https://doi.org/10.1016/j.mssp.2013.06.027)
- Liu, H.; Cao, W.-R.; Su, Y.; Chen, Z.; Wang, Y. *J. Colloid Interface Sci.* **2013**, *398*, 161.
DOI: [10.1016/j.jcis.2013.02.007](https://doi.org/10.1016/j.jcis.2013.02.007)
- Houas, A.; Lachheb, H.; Ksibi, M.; Elaloui, E.; Guillard, C.; Herrmann, J. M. *Applied Catalysis B: Environmental* **2013**, *1*, 145.
DOI: [10.1016/j.apcatb.2013.02.027](https://doi.org/10.1016/j.apcatb.2013.02.027)
- Ramanathan, K.; Contreras, M. A.; Perkins, C. L.; Asher, S.; Hasoon, F. S.; Keane, J.; Young, D.; Romero, M.; Metzger, W.; Noufi, R. *et al. Prog. Photovolt.: Res. Appl.* **2003**, *11*, 225.
DOI: [10.1002/pip.494](https://doi.org/10.1002/pip.494)
- Lo, S.; Liu, Z.; Li, J.; Lai, H. C.; Yan, F. *Progress in Natural Science: Materials International* **2013**, *23*, 514.
DOI: [10.1016/j.pnsc.2013.09.003](https://doi.org/10.1016/j.pnsc.2013.09.003)
- Lin, Z. Q.; Lai, Y. K.; Hu, R. G.; Li, J.; Du, R. G.; Lin, C. J.; *Electrochimica Acta* **2010**, *55*, 8717.
DOI: [10.1016/j.electacta.2010.08.017](https://doi.org/10.1016/j.electacta.2010.08.017)
- Gowda, M. S.; Shiva, P.; Kumar, K.; Kulkarni, R. M. *International Research Journal of Environment Sciences* **2014**, *3*, 20.
- Guerguerian, G.; Elhordoy, F.; Pereyra, C. J.; Marotti, R. E.; Martin, F.; Leinen, D.; Ramos-Barrado, J. R.; Dalchiele, E. A. *Nanotechnology* **2011**, *22*, 505401.
DOI: [10.1088/0957-4484/22/50/505401](https://doi.org/10.1088/0957-4484/22/50/505401)

23. Ramanathan K.; Contreras M. A.; Perkins C. L.; Asher S.; Hasoon F.S.; Keane J.; Young D.; Romero M.; Metzger W.; Noufi R.; *Prog. Photovolt.: Res. Appl.* **2003**, *11*, 225.
DOI: [10.1002/pip.494](https://doi.org/10.1002/pip.494)
24. Wang X.; Liu G.; Lu G. Q.; Cheng H.; *International Journal of Hydrogen Energy* **2010**, *35*, 8199.
DOI: [10.1016/j.ijhydene.2009.12.091](https://doi.org/10.1016/j.ijhydene.2009.12.091)
25. Dai B.; Chao C.; Lu X.; Xia Q.; Han J.; Mao F.; Yang J.; and Sun D.; *Journal of Nanotechnology* **2015**, *1*.
DOI: [10.1155/2015/614170](https://doi.org/10.1155/2015/614170)
26. Jain N.; Bhargava A.; Panwar J.; *Chemical Engineering Journal*, **2014**, *243*, 549.
DOI: [10.1016/j.ccej.2013.11.085](https://doi.org/10.1016/j.ccej.2013.11.085)
27. Liu Y.; Chen X.; Xu Y.; Zhang Q.; and Wang X.; *Journal of Nanomaterials* **2014**, *1*.
DOI: [10.1155/2014/381819](https://doi.org/10.1155/2014/381819)
28. Bhagat U. K.; More P. V. and Khanna P. K.; *SAJ Nanoscience and Nanotechnology* **2015**, *1*, 1.
29. Sapra S.; Nanda J.; Sharma D. D.; EL-AL F. A. and Hodes G.; *Chem. Commun* **2001**, *21*, 2188.
DOI: [10.1039/B106420G](https://doi.org/10.1039/B106420G)
30. Lu L.; Xu X. L.; Liang W. T.; Lu H. F.; *J. Phys. Condens. Matter* **2007**, *19*, 406221.
DOI: [10.1088/0953-8984/19/40/406221](https://doi.org/10.1088/0953-8984/19/40/406221)
31. Tschirner N.; Lange H.; Schliwa A.; Biermann A.; Thomsen C.; Lambert K.; Gomes R.; Hens Z.; *Chem. Mater* **2012**, *24*, 311.
DOI: [10.1021/cm202947n](https://doi.org/10.1021/cm202947n)
32. Azhniuk Y. M.; Milekhin A. G.; Gomonnai A. V.; Lopushansky V. V.; Yukhymchuk V. O.; Schulze S.; Zenkevich E. I.; Zahn D. R. T.; *J. Phys.: Condens. Matter* **2004**, *16*, 9069.
DOI: [10.1088/0953-8984/16/49/022](https://doi.org/10.1088/0953-8984/16/49/022)
33. Sharma M.; Jain T.; Singh S.; Pandey O. P.; *Solar Energy* **2012**, *86*, 626.
DOI: [10.1016/j.solener.2011.11.006](https://doi.org/10.1016/j.solener.2011.11.006)
34. Peng Z.; Tang H.; Tang Y.; Yao K. F.; and Shao H. H.; *International Journal of Photoenergy* **2014**, *9*, 1.
DOI: [10.1155/2014/867565](https://doi.org/10.1155/2014/867565)
35. Soltani N.; Saion E.; Hussein Md. Z.; Erfani M.; Abedini A.; Bahmanrokh G.; Navasery M. and Vaziri P.; *Internal Journal of Molecular Science* **2012**, *13*, 12242.
DOI: [10.3390/ijms131012242](https://doi.org/10.3390/ijms131012242)
36. Lavand A. B.; Malghe Y. S.; *Journal of Saudi Chemical Society* **2015**, 471.
DOI: [10.1016/j.jscs.2015.07.001](https://doi.org/10.1016/j.jscs.2015.07.001)
37. Khanchandani S.; Kundu S.; Patra A.; and Ganguli A. K.; *The Journal of Physical Chemistry C* **2012**, *116*, 23653.
DOI: [10.1021/jp3083419](https://doi.org/10.1021/jp3083419)
38. Desong W.; Zhang J.; Luo Q.; Li X.; Duan Y.; An J.; *Journal of Hazardous Materials* **2009**, *169*, 546.
DOI: [10.1016/j.jhazmat.2009.03.135](https://doi.org/10.1016/j.jhazmat.2009.03.135)
39. Fatin. S. O.; N. Lim H.; Tan W. T.; Huang N. M.; *Int. J. Electrochem. Sci.* **2012**, *7*, 9074.

Advanced Materials Letters

Copyright © 2016 VBRI Press AB, Sweden
www.vbripress.com/aml

A Monthly Journal

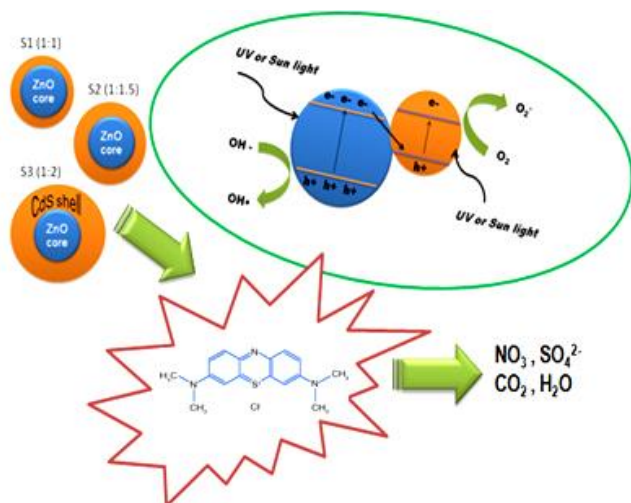
Publish your article in this journal

Advanced Materials Letters is an official international journal of International Association of Advanced Materials (IAAM, www.iaamonline.org) published monthly by VBRI Press AB from Sweden. The journal is intended to provide high-quality peer-review articles in the fascinating field of materials science and technology particularly in the area of structure, synthesis and processing, characterisation, advanced-state properties and applications of materials. All published articles are indexed in various databases and are available download for free. The manuscript management system is completely electronic and has fast and fair peer-review process. The journal includes review article, research article, notes, letter to editor and short communications.



VBRI Press
a rapid publication platform

Graphical Abstract



ZnO/CdS core-shell nanoparticles were synthesized successfully *via* solution chemistry method in aqueous medium by rapid homogenization method. The nanoparticles showed high photocatalytic activity due to the effective charge transfer between two coupled semiconductors. The synthesized ZnO/CdS nanoparticles demonstrated high photocatalytic activity under direct sunlight (81.28 %) however the same was much lower when 8Watt UV lamp was used (35.82 %) for the degradation of methylene blue in aqueous solution. It was observed that the degradation of MB was higher from core/shell nanostructures than and the physical mixture of ZnO-CdS which was prepared separately.

Supplementary Information

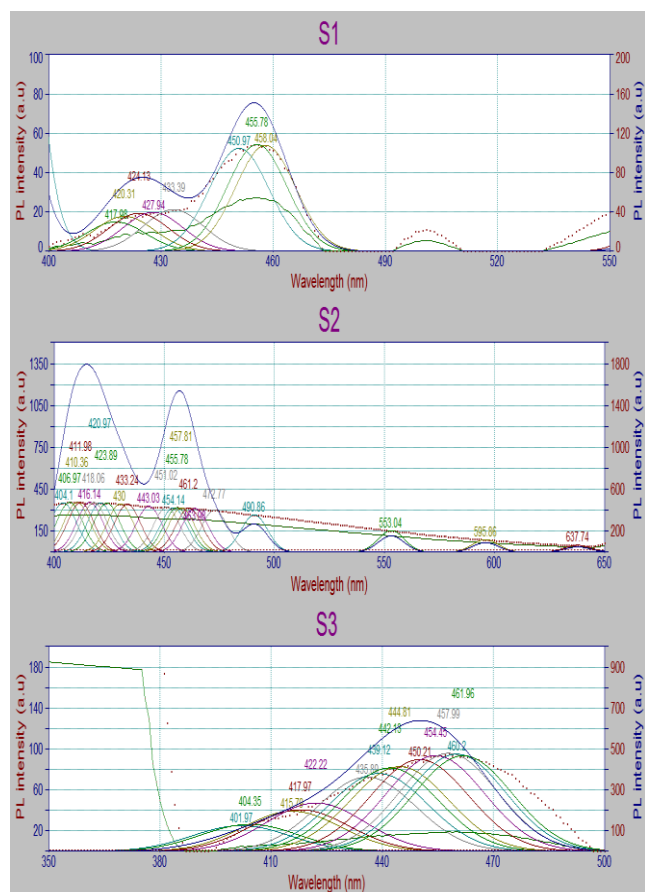


Fig. S.1: Deconvoluted PL spectra of ZnO/CdS core-shell nanostructures where multiple peaks are observed as a part of a broad peak. The broad profile of the PL peak is due to the well known surface related defects occurring in CdS shell.

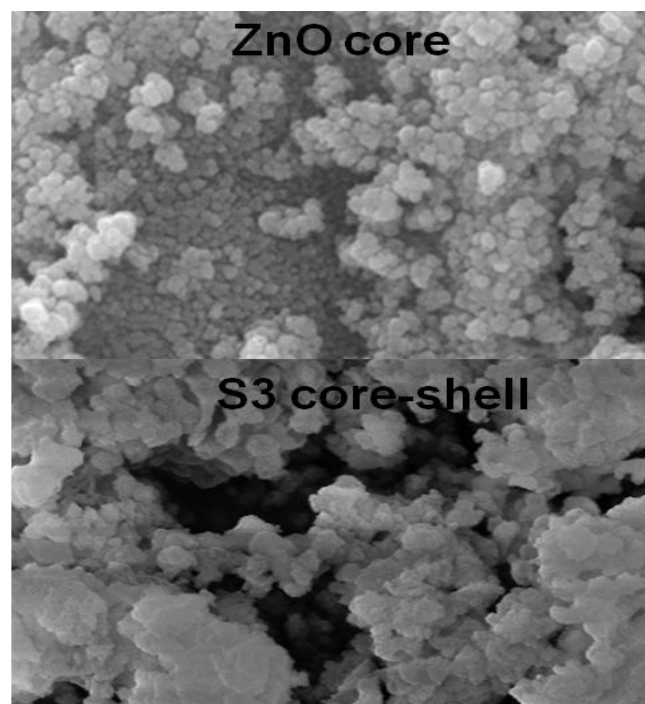


Fig. SI 2: SEM images of ZnO core and S3 core-shell nanostructure.

The amorphous shell formation is clearly visible in the image.

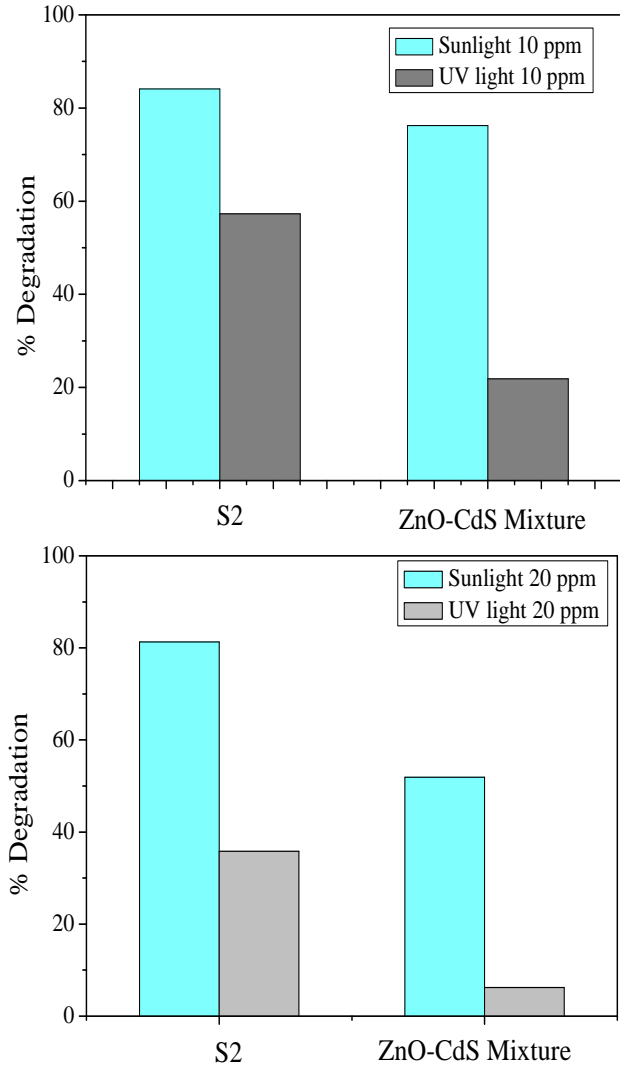


Fig. SI 4. Comparison of degradation (%) for ZnO/CdS (S2) core-shell nanostructure and ZnO-CdS physical mixture.